Chapter 3

Free Motions of a Point-Mass Breakwater

3.1 Introduction

Before more complicated analyses are conducted, a simple study was necessary to see common responses of the breakwater and to check that the formulation was correct. In the first analyses, the breakwater was modeled as a point mass, which would undergo free motion. This point-mass breakwater (PMBW) is an infinitesimally small point of mass m. Free motions are those where the only force acting on the breakwater is gravity, which pulls the breakwater down. Thus, the problem investigated is a two-dimensional free vibration of a point mass which is restricted to a specified region. More realistic and complicated cases will be investigated in subsequent chapters.

3.2 Equations of Motion

The equations of motions (EOM's) developed in Chapter 2 will be used to model the motions of the PMBW in this problem. These EOM's are reviewed in Section 3.5.2.

3.3 Analyzed Cases

Several different cases were analyzed to investigate how the variation of different parameters affected the motions of the breakwater. For this problem, the parameters include the radius of the mooring cables, r, the coefficient of restitution, e, and initial x and y positions and velocities. These parameters and initial conditions are summarized in Table 3.1. This table shows the case number, which was used to identify each case; this number is a series of numbers taken from the initial conditions. In this problem, the case

number uses r, e, x(0), $\dot{x}(0)$, y(0), $\dot{y}(0)$ in this order to identify it. For example, the standard case has a case number of 194611. The standard case will be explained in detail later and is denoted by the shaded cells in Table 3.1 where $v_x = \dot{x}(0)$ and $v_y = \dot{y}(0)$. Further, the initial conditions shown in this table are put into a series of groups. These groups were used to see how varying only one parameter would affect the breakwater's response. These series and the extra cases analyzed that do not necessarily fall directly into a series were used to decide ranges of parameters to be used in future analyses.

Table 3.1. Parameters and Initial Conditions for Free Motions of a Point-Mass Breakwater

Case #						
rexv$_x$yv$_y$	**r**	**e**	**x**	**v$_x$**	**y**	**v$_y$**
r						
294611	2.5	0.9	0.4	0.6	1.0	-0.1
194611	1.5	0.9	0.4	0.6	1.0	-0.1
292010	2.5	0.9	0.2	0.0	1.0	0.0
192010	1.5	0.9	0.2	0.0	1.0	0.0
e						
114611	1.5	1.0	0.4	0.6	1.0	-0.1
194611	1.5	0.9	0.4	0.6	1.0	-0.1
174611	1.5	0.7	0.4	0.6	1.0	-0.1
154611	1.5	0.5	0.4	0.6	1.0	-0.1
174010	1.5	0.7	0.4	0.0	1.0	0.0
164010	1.5	0.6	0.4	0.0	1.0	0.0
154010	1.5	0.5	0.4	0.0	1.0	0.0
x						
194010	1.5	0.9	0.4	0.0	1.0	0.0
174010	1.5	0.7	0.4	0.0	1.0	0.0
173010	1.5	0.7	0.3	0.0	1.0	0.0
172010	1.5	0.7	0.2	0.0	1.0	0.0
171010	1.5	0.7	0.1	0.0	1.0	0.0
r, e, x						
2751010	2.5	0.75	1.0	0.0	1.4	0.0
272010	2.5	0.7	0.2	0.0	1.0	0.0
264010	2.5	0.6	0.4	0.0	1.0	0.0
261010	2.5	0.6	1.0	0.0	1.4	0.0
194611m (mirror)	1.5	0.9	-0.4	-0.6	1.0	-0.1

3.3.1 Standard Case

A standard case was developed for this problem as a starting point for the variation of parameters. The standard parameters and initial conditions for this PMBW problem are:

$$r=1.5 \qquad e=0.9$$

$$x(0)=0.4 \qquad \dot{x}(0) = 0.6 \qquad (3.1)$$

$$y(0)=1.0 \qquad \dot{y}(0) = -0.1$$

The PMBW is given initial x and y positions, denoted by I in Fig. 3.1, in the top right corner of the region. This position was chosen because the only force in the system was the gravitational force, and thus if the PMBW was given an initial position near its equilibrium state then it would not likely have long-lasting motions. In other words, the PMBW has potential energy and no kinetic energy added to the system by some outside force. Theoretically the PMBW will settle to the bottom of the region because it loses energy every time it impacts a boundary. If the PMBW is given a low initial height, then it will settle quicker than if it is started higher, and the primary purpose of this problem is to investigate the response of the breakwater. The longer the PMBW continues moving, the more characteristic responses may be seen from its motion, and thus the PMBW will be started at a higher position.

3.4 Analysis of Data

The data collected was analyzed to see what types of behavior the PMBW exhibited during its period in motion. The primary method of evaluating the response of the PMBW was to produce and evaluate several types of graphs.

3.4.1 Types of Graphs

By putting the data into graphical form, it was easy to interpret the responses of the PMBW. The trajectory plot is used to show the motion of the breakwater in a planar

form with the breakwater bouncing between two circular arc boundaries. The boundaries are definite (i.e., fixed in space) in the point-mass cases and are drawn on the plot. Figure 3.1 shows a typical trajectory plot with I denoting the initial point. Figure 3.2 shows a plot of normal velocity just before impact vs. time. This plot is used to show how the normal velocity (snap loading) tends to decrease throughout time due to a loss of energy. Vertical lines are drawn below the points (denoted by x's) corresponding to impacts with the right circular arc in Fig. 3.1, this was done to help show when they occur relative to impacts with the left circular arc (denoted by o's). After the first few impacts, the circles are higher than the x's and almost seem to lie on a smooth curve in this case. Theoretically, the motion will die out with an infinite number of impacts in a finite time. Other plots produced include: x and y vs. time for time histories; x and y velocity vs. x and y position, respectively, for phase diagrams; impact Poincaré plots; and total and kinetic energy vs. time plots. Though several graphs were produced, the trajectory and normal velocity before impact vs. time plots were the most useful for the analyses being performed. Some of the other plots are shown in the Appendix.

3.4.2 Observations

After varying the different parameters of the problem, several characteristic phenomena were observed about the motions of a PMBW. The following is a summary of these observations.

The radius was the first parameter varied to see how the PMBW would respond. There does not appear to be a significant difference between the motions of a case that has a radius of 1.5 and a case that has a radius of 2.5. The only notable difference between the two radii is the ability for the PMBW to bounce around longer and travel about higher portions of the region more with the r=2.5 cases. Figures 3.3 and 3.4 illustrate this difference in size and range of motions of the PMBW dependent upon the mooring line radius. Note that the Figs. 3.3 and 3.4 are approximately to scale.

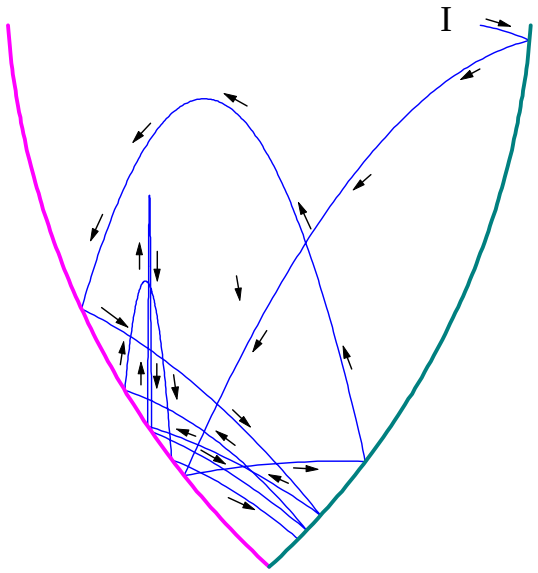

Fig. 3.1. Typical Trajectory Plot, Standard Case

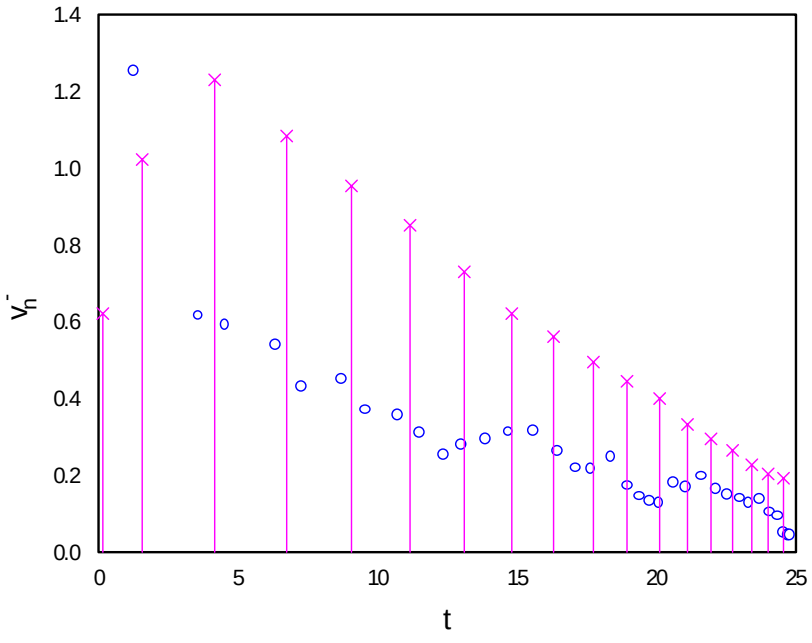

Fig. 3.2. Typical Normal Velocity Before Impact vs. Time, Standard Case

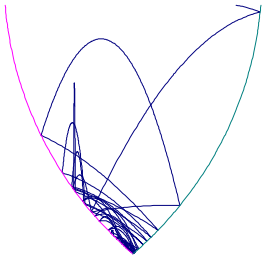

Fig. 3.3. y vs. x, Case 194611 (r=1.5)

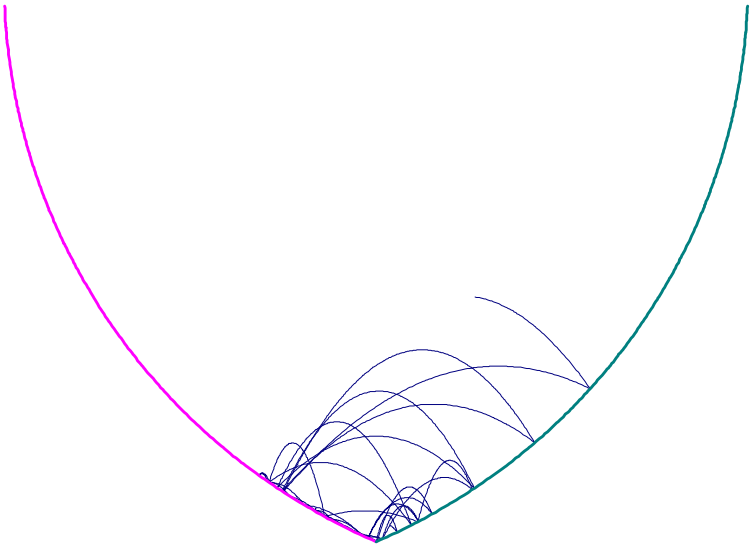

Fig. 3.4. y vs. x, Case 294611 (r=2.5)

The lower the coefficient of restitution, the quicker the PMBW dies out to the bottom of the region. This is demonstrated in Figs. 3.5-3.7, where it can be seen that as the coefficient of restitution is decreased from 0.9 to 0.7 to 0.5, the time it takes for the PMBW to lose enough energy to settle to the bottom of the region is reduced. The breakwater will travel around the region until it loses enough energy to die down. The graph of the case where e=1.0 is not shown in this series, because in this case the PMBW retained so much energy that its motions caused it to go above the upper boundary, y=h, which indicates, in reality, that the breakwater hits the sea bed. The trajectory is shown in Fig. 3.8 and reaches y=h at point A. This motion is undesired and most likely not possible.

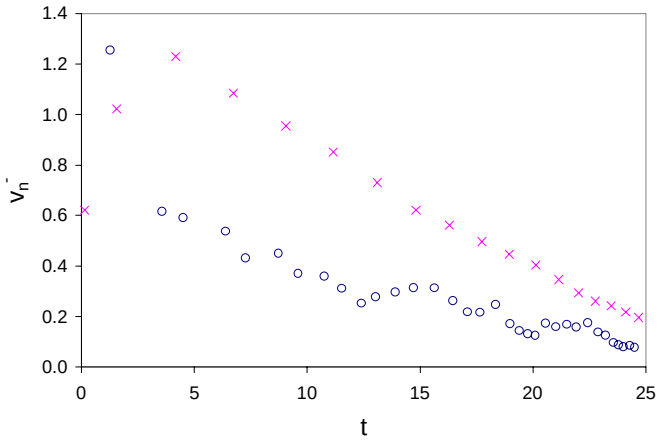

Fig. 3.5. v_n^- vs. t, Case 194611 (e=0.9)

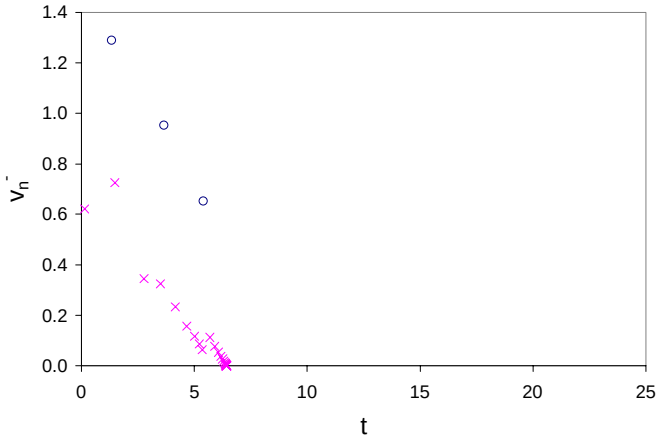

Fig. 3.6. v_n^- vs. t, Case 174611 (e=0.7)

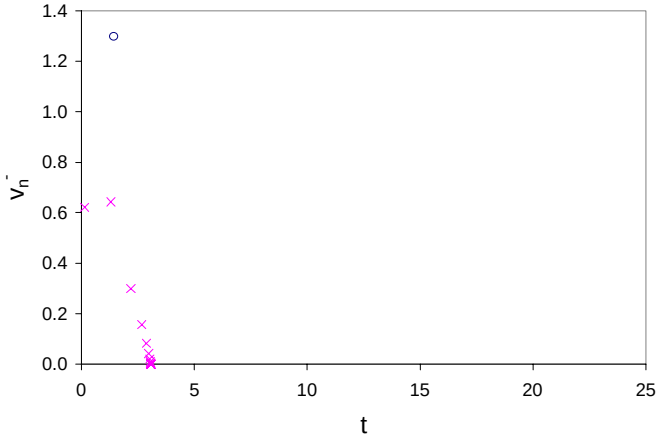

Fig. 3.7. v_n^- vs. t, Case 154611 (e=0.5)

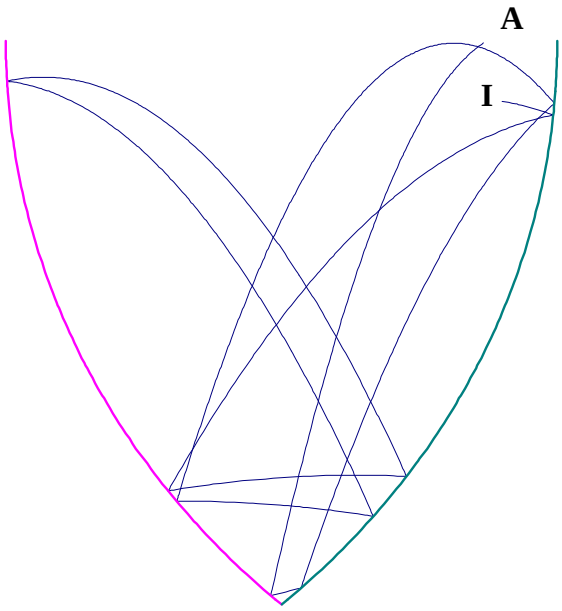

Fig. 3.8. y vs. x, Case 114611 (e=1.0)

When the breakwater is started on one side of the axis of symmetry, it tends to hit the boundary on the other side with a greater normal velocity than the boundary on the side on which it started. This is due to the curvature of the opposite boundary and the angle at which it strikes; when the PMBW hits the boundary at almost a right angle to the slope of the curve, the impact velocity is high. Conversely, the normal velocity would be low if the breakwater just grazes off of a boundary and does not hit it straight on, thus transferring less normal velocity. The magnitude of the normal velocity is dependent upon the direction of the PMBW trajectory relative to the tangent to the boundary curve where the breakwater hits. As seen in Fig. 3.2, the normal velocity usually decreases in magnitude because it loses energy as it impacts. However, the possibility of a PMBW with a normal velocity greater than a prior normal velocity exists. This is because if the breakwater travels downwards for a long time, it gains velocity from gravitational acceleration and possesses more kinetic energy and may have a large normal velocity at impact, even if the breakwater does not hit at a right angle and only grazes a boundary. The normal velocities tend to die down with time because of the coefficient of restitution, which removes energy from the system, as seen in a typical v_n^- vs. t plot in Fig 3.2. Some trials hardly get started before they die out due to initial conditions or to a low coefficient

of restitution. The above said phenomenon may be seen in comparing how the breakwater strikes a boundary in Fig. 3.1 to the magnitude of the normal velocity in Fig. 3.2. Section 3.5.3 discusses this phenomenon further.

The more energy you add to the system, like increasing the x and y velocities, the more excited the motion of the breakwater may be. This can be seen in Figs. 3.9 and 3.10, where in Fig. 3.9 the breakwater is started with some velocities while in Fig. 3.10 the breakwater is essentially dropped from rest. In Fig. 3.9 the PMBW moves about the region striking both boundaries, while the PMBW in Fig. 3.10 mainly sticks close to the right boundary because it has less horizontal velocity to cause it to strike the left boundary.

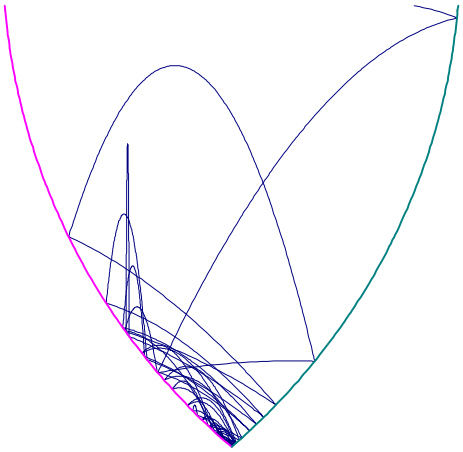

Fig. 3.9. y vs. x, Case 194611
(v_x= 0.6, v_y= -0.1)

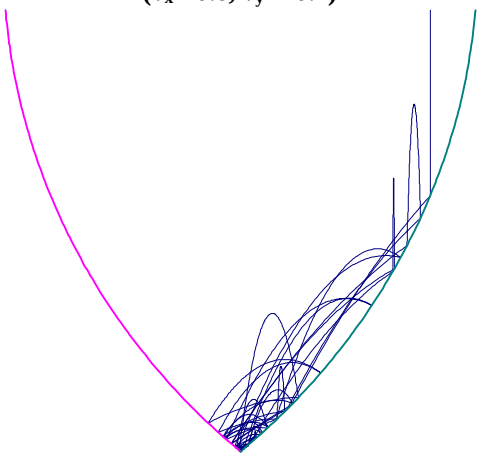

Fig. 3.10. y vs. x, Case 194010
(v_x= 0.0, v_y= 0.0)

3.5 Verification of Computer Modeling Techniques

After a solution procedure was developed and coded into a computer program, several cases were investigated. To verify that the formulation and coding were correct, a few checks were developed to determine the accuracy and versatility of the formulation. This was done using data collected from the cases investigated.

3.5.1 Analytical vs. Numerical Solution

As seen in Chapter 2, the bases for the motions of the PMBW are the classical physics equations of motion. For this first problem investigated, numerical integration was used to solve the equations of motion. However, a numerical solution is not necessary in this case since an analytical solution exists. A numerical solution was first developed for the first problem to give a check on the solution process and for reference to future researchers. One can solve for the motions of the PMBW by hand or with a numerical method. A comparison of the numerical solution to the analytical solution was investigated. This was done to determine the accuracy of the numerical modeling program using the DIVPAG subroutine from IMSL. The comparison of the two solution methods is best performed on the impact times. Most of the error will accumulate in the convergence rather than in the straight numerical integration of the free motions between impacts.

3.5.2 Verification of Impact Times

Once data was collected for a case using the numerical solution, in this instance the standard case, it was then compared with an analytical solution developed to determine the impact times. Two solution procedures were used and compared to the numerical solution. Both procedures used the same analytical solution formulation; the only difference was in the tools used to solve the analytical solution. These tools will be explained later. The following is the formulation of the impact time analytical solution.

To allow us to find the times at which a boundary is hit, the following formulation was developed. First, the EOM's for the free motion case, Equations 3.2-3.7, are combined with the equations for the g_1=0 and g_2=0 boundaries, Equations 3.12 and 3.13, as seen in Equation 3.14:

$$x = c_2 t + c_1 \qquad y = -\tfrac{1}{2} t^2 + c_4 t + c_3 \qquad (3.2, 3.3)$$

$$\dot{x} = c_2 \qquad \dot{y} = -t + c_4 \qquad (3.4, 3.5)$$

$$\ddot{x} = 0 \qquad \ddot{y} = -1 \qquad (3.6, 3.7)$$

where the constants for motion following $t=t_i$ (initial time or impact time) are

$$c_1 = x_i - c_2 t_i \qquad c_3 = y_i - c_4 t_i + \tfrac{1}{2} t_i^2 \qquad (3.8, 3.9)$$

$$c_2 = \dot{x}_i \qquad c_4 = \dot{y}_i + t_i \qquad (3.10, 3.11)$$

The boundary equations g_1 and g_2 are

$$g_1=(x-1)^2 + (y-h)^2 - r^2 \qquad g_2=(x+1)^2 + (y-h)^2 - r^2 \qquad (3.12, 3.13)$$

Plugging x and y into the g_1=0 equation gives

$$\left[x_i + \dot{x}_i (t - t_i) - 1\right]^2 + \left[y_i + \dot{y}_i (t - t_i) - \tfrac{1}{2}(t - t_i)^2 - h\right]^2 = r^2 \qquad (3.14)$$

Rearranging and simplifying gives

$$\left[x_i - \dot{x}_i t_i - 1 + \dot{x}_i t\right]^2 + \left[y_i - \dot{y}_i t_i - \tfrac{1}{2} t_i^{\,2} - h + (\dot{y}_i + t_i) t - \tfrac{1}{2} t^2\right]^2 - r^2 = 0 \qquad (3.15)$$

After expanding, the following constants are defined:

$$A_1 = x_i - \dot{x}_i t_i - 1 \qquad (3.16)$$

$$B = \dot{x}_i \qquad (3.17)$$

$$C = y_i - \dot{y}_i t_i - \tfrac{1}{2} t_i^2 - h \qquad (3.18)$$

$$D = \dot{y}_i + t_i \qquad (3.19)$$

$$E = -\tfrac{1}{2} \qquad (3.20)$$

Similarly, plugging x and y into g_2=0 gives

$$A_2 = x_i - \dot{x}_i t_i + 1 \tag{3.21}$$

The rest of the constants B, C, D, E are the same for $g_2=0$ as for $g_1=0$.

Next, by plugging the constants back into the boundary equations for $g_1=0$ and $g_2=0$, the general Equation 3.22 is developed:

$$g_{(1,2)} = C_o + C_1 t + C_2 t^2 + C_3 t^3 + C_4 t^4 = 0 \tag{3.22}$$

where

$$C_o = A_{(1,2)}^2 + C^2 - r^2 \tag{3.23}$$

$$C_1 = 2A_{(1,2)}B + 2CD \tag{3.24}$$

$$C_2 = B^2 + 2CE + D^2 \tag{3.25}$$

$$C_3 = 2DE \tag{3.26}$$

$$C_4 = E^2 \tag{3.27}$$

By solving Equation 3.22, the times when $g_1=0$ and $g_2=0$ may be computed. The impact time analytical solution is obtained from this equation by using the following procedure:

1. plug the initial conditions into the coefficient equations, Equations 3.16-3.21 and 3.23-3.27, for the particular boundary being investigated;
2. plug the coefficients into the fourth-order equation, Equation 3.22;
3. solve Equation 3.22 with a polynomial equation solver to get an impact time;
4. determine new "initial conditions" following this impact time and then the procedure starts over with step 1 to calculate the subsequent motion and the next impact time.

The first solution procedure used to solve for the impact times involved using Microsoft EXCEL to find the polynomial coefficients and the root finding program on a TI-85 hand calculator. The second solution procedure used Müller's Method of the DZREAL subroutine in the IMSL library to find the root. Both methods used double precision to help control accuracy. These methods only looked at the conditions at the time of impact (i.e., a taut cable) and not at the conditions when both cables were slack because it is believed that during an impact is where the most errors will occur. The results of this

comparison may be seen in Table 3.2, where “Tol” refers to the tolerance and “Diff.” refers to the difference. Further, the values in the table have eight decimal places in order to save space; in actuality, the calculations were performed with numbers having 16 decimal places (double precision).

It must be mentioned that the impact times associated with the DIVPAG solution were computed using the *Regula Falsi* convergence method (Johnson and Riess 1982). From the table we can see that errors accumulate as time goes on. However, the methods of solving for the true impact times are accurate within acceptable tolerances and the numerical solution using DIVPAG matches well with the analytical solution. In Table 3.2 the shaded cells indicate a point where the accuracy drops one order of magnitude.

Table 3.2. Comparison of Impact Times Calculated by Different Methods

Impact #	Impact Times, (DIVPAG) Tol=1.0E-6	Impact Times, (DZREAL) Tol=1.0E-12	Impact Times, (TI-85/Excel) Tol=unknown	Diff. DZREAL-DIVPAG	Diff. DIVPAG-TI-85	Diff. DZREAL-TI-85
0	0.00000000	0.00000000	0.00000000			
1	0.15487522	0.15487524	0.15487524	1.2E-08	1.2E-08	2.7E-13
2	1.29044703	1.29044704	1.29044704	5.4E-09	5.4E-09	1.4E-13
3	1.56122317	1.56122317	1.56122317	2.1E-09	2.1E-09	3.4E-12
4	3.59966608	3.59966598	3.59966598	9.9E-08	9.9E-08	4.0E-11
5	4.17157260	4.17157267	4.17157267	7.1E-08	7.1E-08	2.8E-12
6	4.52925467	4.52925457	4.52925457	9.9E-08	9.9E-08	8.8E-11
7	6.38741123	6.38741097	6.38741097	2.6E-07	2.6E-07	3.3E-10
8	6.73907649	6.73907664	6.73907664	1.5E-07	1.5E-07	2.4E-12
9	7.28300933	7.28300867	7.28300867	6.6E-07	6.6E-07	1.2E-09
10	8.73095524	8.73095452	8.73095452	7.2E-07	7.1E-07	3.1E-09
11	9.05636623	9.05636656	9.05636656	3.3E-07	3.3E-07	2.0E-10
12	9.59914050	9.59913850	9.59913851	2.0E-06	2.0E-06	7.4E-09
13	10.76988925	10.76988608	10.76988608	3.2E-06	3.2E-06	6.0E-09
14	11.16521568	11.16521650	11.16521650	8.2E-07	8.2E-07	1.7E-09
15	11.53959696	11.53959143	11.53959144	5.5E-06	5.5E-06	1.1E-08
16	12.41141812	12.41140590	12.41140594	1.2E-05	1.2E-05	3.4E-08
17	13.03986820	13.03985781	13.03985784	1.0E-05	1.0E-05	2.3E-08
18	13.10760818	13.10761069	13.10761065	2.5E-06	2.5E-06	4.1E-08
19	13.91268806	13.91264917	13.91264933	3.9E-05	3.9E-05	1.6E-07
20	14.72034117	14.72030045	14.72030060	4.1E-05	4.1E-05	1.5E-07
21	14.81818740	14.81819959	14.81819948	1.2E-05	1.2E-05	1.1E-07
22	15.64892103	15.64878279	15.64878340	1.4E-04	1.4E-04	6.2E-07
23	16.30909588	16.30913839	16.30913814	4.3E-05	4.2E-05	2.4E-07
24	16.46689858	16.46670330	16.46670420	2.0E-04	1.9E-04	9.0E-07
25	17.10958634	17.10908788	17.10909025	5.0E-04	5.0E-04	2.4E-06
26	17.66412876	17.66356037	17.66356306	5.7E-04	5.7E-04	2.7E-06
27	17.73239474	17.73255352	17.73255277	1.6E-04	1.6E-04	7.5E-07
28	18.37584603	18.37433473	18.37434191	1.5E-03	1.5E-03	7.2E-06
29	18.94699238	18.94757767	18.94757495	5.9E-04	5.8E-04	2.7E-06
30	19.01118237	19.00810018	19.00811490	3.1E-03	3.1E-03	1.5E-05
31	19.41265035	19.40475649	19.40479420	7.9E-03	7.9E-03	3.8E-05
32	19.79233780	19.78092566	19.78098028	1.1E-02	1.1E-02	5.5E-05
33	20.10826357	20.09518713	20.09524977	1.3E-02	1.3E-02	6.3E-05
34	20.12473656	20.12721416	20.12720271	2.5E-03	2.5E-03	1.1E-05
35	20.61283111	20.58340792	20.58354735	2.9E-02	2.9E-02	1.4E-04
36	21.06461945	21.02023927	21.02045245	4.4E-02	4.4E-02	2.1E-04
37	21.12226038	21.13614937	21.13608828	1.4E-02	1.4E-02	6.1E-05
38	21.62245445	21.52829593	21.52873485	9.4E-02	9.4E-02	4.4E-04
39	21.95838994	22.00416803	22.00397907	4.6E-02	4.6E-02	1.9E-04

3.5.3 Verification of Rebound Angles

When the cable becomes taut, the x and y positions are assumed to remain the same before and after the impact. After the positions have been converged within the tolerance, then the velocities are changed according to the geometry of the angle at which the PMBW strikes the boundary. The magnitude of the normal velocity (snap loading) is based on the angle at which the boundary is hit. The more perpendicular the angle of strike, the higher the value of normal velocity. More extensively, as in the physics of an impact, the angles at which an object strikes and rebounds off another object should be on opposite sides of a perpendicular to the point on the boundary at which the object strikes. Thus, the following check was created to prove that the angles at which the breakwater strikes and rebounds off a boundary are on opposite sides of a perpendicular to the boundary. This shall be done by investigating the striking and rebounding angles of the boundary $g_2=0$. As seen in Figs. 3.11 and 3.12, the angle ψ, which is measured from the horizontal to the boundary, has $\pi/2$ added to it to give an angle perpendicular to the boundary and measured from the horizontal. From this angle, striking and rebounding angles should be on either side of this perpendicular.

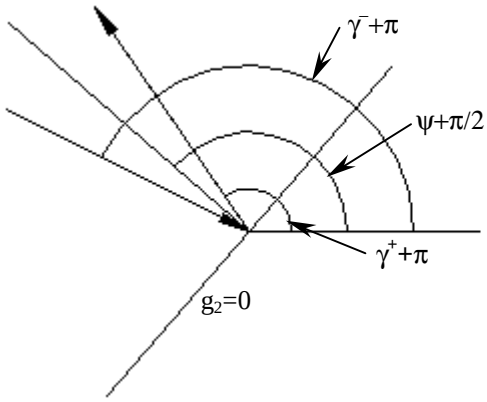

Fig. 3.11. Breakwater Striking Upwards

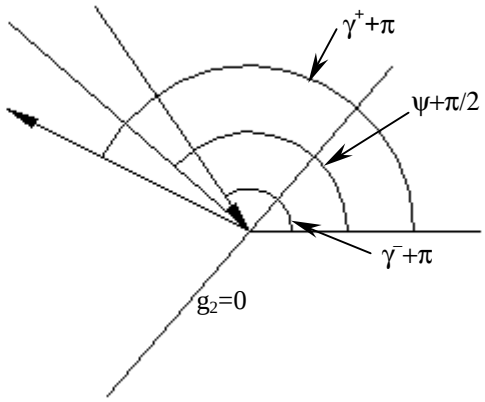

Fig. 3.12. Breakwater Striking Downwards

The superscript (-) denotes quantities just before impact and the superscript (+) denotes quantities just after impact.

To verify this conclusion, the following criteria must be met:

$$\gamma^{-}+\pi > \psi+\pi/2 > \gamma^{+}+\pi \tag{3.28}$$

where ψ may be obtained from Section 2.5.3.1 and

$$\gamma^{-} = \tan^{-1}\left(\frac{\dot{y}^{-}}{\dot{x}^{-}}\right) \tag{3.29}$$

Similarly, to get γ^{+} just replace the (-) superscripts with (+) in Equation 3.29.

Table 3.3 shows results from an impact during the standard case.

Table 3.3. Verification of Striking and Rebound Angles

Impact Time	11.16521661				
	x	**v_x**	**v_y**	**γ**	**$\gamma+\pi$**
before (-)	0.03969501	0.58081667	-0.62245686	-0.81999012	2.32160253
after (+)	0.03969501	-0.54024265	0.54337590	-0.78828962	2.35330303
ψ	0.76582237				
$\psi+\pi/2$	2.33661870				
		Difference			
$\gamma^{-}+\pi$	2.32160253	0.015016166			
$\psi+\pi/2$	2.33661870				
$\gamma^{+}+\pi$	2.35330303	0.016684334			
γ^{+}/γ^{-}	0.900015867				

By obtaining the positions and velocities before and after the impact, one can calculate the values of ψ, γ^{-}, and γ^{+} and after adding the appropriate angles to these, one can compare the angles as measured from the horizontal x-axis. One can see that, in this case, $\gamma^{-}+\pi < \psi+\pi/2 < \gamma^{+}+\pi$. Furthermore, it can be seen, within some error, that γ^{+}/γ^{-} is the coefficient of restitution, which is 0.9 for the standard case. Lastly, it may be noted that the angle between the velocity vector and the perpendicular is greater after impact than before. This is due to loss of energy based on the coefficient of restitution (i.e., the breakwater does not have the same energy before and after impact, so it will not rebound as high).

3.5.4 Verification of Impact Conditions

The trials were all started from the same side of the axis of symmetry and same y position, as seen in Table 3.1. If one were to start the trial on the opposite side by changing the signs of the x values of the initial conditions, then a mirror image of the trial would occur. This indicates that both of the derivations of the convergence and rebounding during an impact are correct. This mirroring is about the middle axis of the trajectory plot (Figs. 3.13 and 3.14) at x=0 or the axis of symmetry for the valley trajectory plots between g_1=0 and g_2=0.

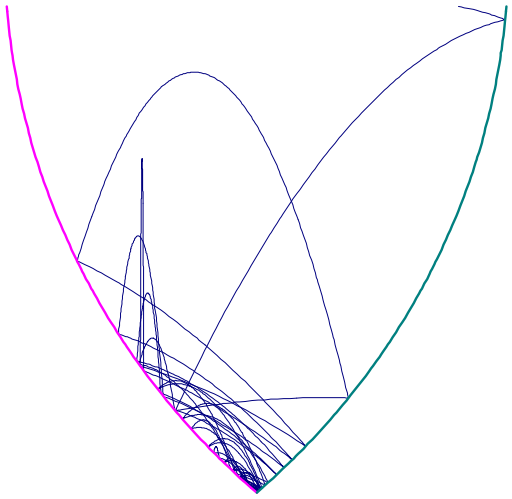

Fig. 3.13. y vs. x, Standard Case (Case 194611)

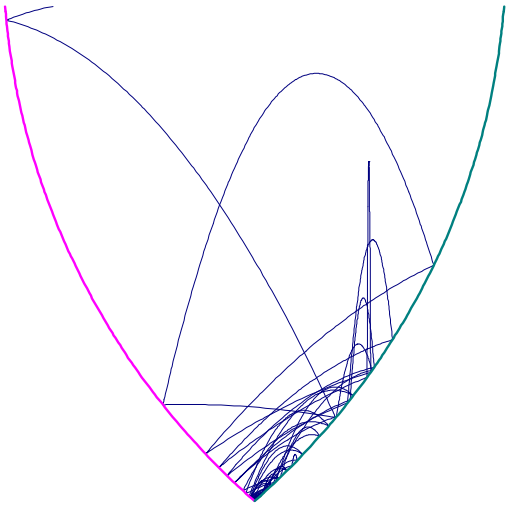

Fig. 3.14. y vs. x, Mirror of Standard Case